Rev. Mexicana Astron. Astrof., **22**, 285-296 (1991)

SCATTERED LIGHT IN M8[1]

L.J. Sánchez and M. Peimbert[2]

Instituto de Astronomía
Universidad Nacional Autónoma de México

Received 1991 May 15

RESUMEN

Se presenta espectrofotometría en el intervalo de 3400 a 7400 A para seis áreas en la nebulosa de la Laguna. Se determinó la contribución atómica al continuo en emisión y se encontró que más de la mitad del continuo se debe a luz dispersada por partículas de polvo. En la dirección del Reloj de Arena se detectaron las líneas $\lambda\lambda$4200 y 4686 de He^+ en absorción; este resultado también implica que la mayor parte del continuo en dicha dirección es debido a luz dispersada por polvo, como es el caso en las nebulosas de reflexión. El cociente efectivo de gas a polvo ($N_H/N_d\sigma_d$) en la dirección del Reloj de Arena se determinó a partir de dos métodos diferentes.

ABSTRACT

Spectrophotometry in the 3400 to 7400 A range is presented for six areas inside the Lagoon nebula. We have derived the electron temperature, the electron density and the $N(He^+)/N(H^+)$ abundance ratios to determine the atomic contribution to the continuum emission. We have found that more than half of the continuum emission is due to dust scattered light. In the direction of the Hourglass we have detected the $\lambda\lambda$4200 and 4686 He^+ lines in absorption; this result also implies that most of the continuum emission in that direction is produced by dust scattered light as in reflection nebulae. The effective gas to dust ratio ($N_H/N_d\sigma_d$) in the direction of the Hourglass was determined from two different methods.

Key words: **INTERSTELLAR-DUST – NEBULAE-H II REGIONS – NEBULAE-REFLECTION**

I. INTRODUCTION

O'Dell and Hubbard (1965) and O'Dell, Hubbard, and Peimbert (1966) showed that most of the continuum observed in the visual range of the spectrum of H II regions is due to dust scattered light. Peimbert and Goldsmith (1972) detected the λ4686 line of He^+ in absorption in the continuum emission from the Orion Nebula confirming the conclusion derived by O'Dell and Hubbard and O'Dell *et al.*.

M8, also known as NGC 6523, S25, W29 and the Lagoon nebula, is one of the most studied galactic H II regions. The H II region forms a blister on the surface of a giant molecular cloud that is located behind the H II region (e.g., Lada *et al.* 1976). The open cluster NGC 6530 is embedded in M8, the brightest regions of M8 are to the west of NGC 6530. Most of the ionization of M8 is due to three O stars 9 Sgr (HD 164794), HD 165052 and Herschel 36 (H36, HD 164740).

We decided to study the continuum emission from the brightest regions of M8 to try to: a) search for He^+ lines in absorption, b) estimate the fraction of the continuum due to dust scattered light, c) determine $N_H/N_d\sigma_d$, the number of H atoms per cm^2 of dust absorption, which has often been called in the literature the effective gas to dust ratio (e.g., O'Dell and Hubbard 1965, O'Dell *et al.* 1966), and d) improve our knowledge on the structure of M8.

1. Partially based on observations collected at the Observatorio Astronómico Nacional of San Pédro Mártir, B.C., México.

2. Visiting Astronomer, KPNO, National Optical Astronomical Observatories, operated by the Association of Universites for Research in Astronomy, Inc., under contract with the National Science Foundation.

II. OBSERVATIONS

a) *2.1-m Telescope at KPNO*

The observations were carried out during May 1978 with the Gold spectrograph and the intensified image dissector scanner (IDS). The IDS is a dual-beam multichannel spectrometer, each spectrum of roughly 20 mm is recorded into 1024 channels. The full width at half-maximum was of 3.8 channels.

Two gratings were used that covered the following wavelength ranges: λλ3400-5200 and λλ5600-7400. The dual entrance slits used were 0.30 × 0.98 mm where the first value is along and the second is perpendicular to the dispersion; they correspond to 3.8" × 12.4" on the plane of the sky. The separation between the center of the slits was 99" on the sky. Each beam was treated independently and in all cases the sky was subtracted from the source. The sky measurements were made outside the body of M8.

The observed regions are shown in Figure 1 (Plate); details are presented in Table 1 and Figure 1. The data were reduced to absolute fluxes using the standard stars observed by Stone (1977) and Oke (1974) and corrected for the nonlinearity of the detector by considering that the actual flux, F, is related to the instrumental signal, S, by (Peimbert and Torres-Peimbert 1987)

$$S \propto F^{1.07}. \qquad (1)$$

TABLE 1

OBSERVED REGIONS

Designation	Location
M8 HG	12" S of center of Hourglass
M8 HGE	99"E of M8 HG
M8 HGW	99"W of M8 HG
M8 1	90"S and 175"W of 9 Sgr
M8 1E	99"E of M8 1
M8 1W	99"W of M8 1
M8 I[a]	90"S and 175"W of 9 Sgr

a. Observed by Peimbert and Costero 1969.

In Table 2 we present the intrinsic line intensities in ergs $cm^{-2}s^{-1}$, $I(\lambda)$, relative to $I(H\beta)$ given by

$$\log\,[I(\lambda)/I(H\beta)] = \log\,[F(\lambda)/F(H\beta)] + C(H\beta)g(\lambda) \quad , \qquad (2)$$

where $F(\lambda)$ is the observed line flux corrected for atmospheric extinction, $C(H\beta)$ is the logarithmic reddening correction at $H\beta$ and $g(\lambda)$ is the reddening function normalized at $H\beta$. The continuum contribution to each emission line was subtracted and was estimated by interpolating the continuum values on both sides of the line.

TABLE 2

LINE INTENSITIES

λ	ID	$g(\lambda)$	$g'(\lambda)$	HG	HGE	HGW	1	1E	1W
3727	[O II]	+0.315	+0.19	+0.44	+0.14	+0.28	−0.02	+0.11	+0.21
3798	H 10	+0.290	+0.17	−1.30	−1.32	−1.30	−1.35	−1.36	−1.31
3835	H 9	+0.280	+0.16	−1.16	−1.14	−1.20	−1.19	−1.14	−1.15
4102	Hδ	+0.200	+0.13	−0.61	−0.64	−0.60	−0.57	−0.65	−0.62
4340	Hγ	+0.135	+0.09	−0.33	−0.34	−0.35	−0.34	−0.34	−0.31
4363	[O III]	+0.130	+0.09	−2.44	−2.07:	...	−2.10:	−2.14:	−2.07:
4472	He I	+0.105	+0.07	−1.47	−1.31	−1.48	−1.33	−1.36	−1.34
4861	Hβ	0.000	0.00	0.00	0.00	0.00	0.00	0.00	0.00
4959	[O III]	−0.020	−0.01	−0.48	−0.16	−0.46	−0.03	−0.15	−0.05
5007	[O III]	−1.030	−0.02	−0.02	+0.36	−0.06	+0.45	+0.37	+0.38
5755	[N II]	−0.190	−0.14	−1.98	...	...	...	...	...
6548	[N II]	−0.330	−0.25	−0.40	−0.86	−0.51	−0.87	−0.85	−0.66
6563	Hα	−0.335	−0.25	+0.45	+0.45	+0.45	+0.45	+0.45	+0.45
6583	[N II]	−0.340	−0.25	+0.14	−0.43	−0.05	−0.43	−0.41	−0.16
6717	[S II]	−0.370	−0.28	−1.08	−1.15	−0.87	−1.19	−1.13	−0.98
6731	[S II]	−0.370	−0.28	−0.91	−1.31	−0.89	−1.24	−1.25	−0.94
$C(H\beta)$				1.00	0.40	0.45	0.15	0.30	0.45
$\log F(H\beta)$				−11.24	−12.49	−12.11	−12.37	−12.50	−12.17

In Table 2 we present two different reddening functions: a) $g(\lambda)$ derived from the normal extinction law (Whitford 1958), that corresponds to a total to selective extinction ratio, R, equal to 3.1, and b) $g'(\lambda)$ derived by Mathis (1990) for R = 5.0. With the exception of M8 HG all the other observed regions are mainly ionized by 9 Sgr and most of their reddening is due to foreground interstellar dust (e.g., Hecht *et al.* 1982 and references therein), therefore for all of them we adopted the normal reddening function. M8 HG is mainly ionized by H36 (see §V) and shows considerably higher extinction than the other observed regions, and it has been found that for H36 R is equal to 4.6 (Hecht *et al.* 1982) or 5.3 (Mathis 1990); consequently to correct the M8 HG observations we will adopt the reddening function for R = 5.0. Fortunately after correcting for reddening, the line intensity ratios in the visual region are almost unaffected by deviations from the normal extinction law; alternatively the $C(\mathrm{H}\beta)$ changes are significant and are proportional to the ratio of the R values.

The $C(\mathrm{H}\beta)$ values were obtained by fitting the observed $H\gamma/\mathrm{H}\beta$ and $\mathrm{H}\delta/\mathrm{H}\beta$ ratios to the theoretical ones computed by Hummer and Storey (1987) for T_e = 10 000 K and N_e = 100 cm^{-3}, which are very similar to those computed by Brocklehurst (1971). We compared the free-free emission of M8 HG from the work by Woodward *et al.* (1986), that for T_e = 8 000 K amounts to an emission measure of 1.29×10^6 cm^{-6} pc, with the $F(\mathrm{H}\beta)$ value in Table 2 and obtained $C(\mathrm{H}\beta) = 0.96 \pm 0.10$ in excellent agreement with the value derived from the Balmer decrement.

Since the blue and the red part of the spectrum were not observed simultaneously the $I(\mathrm{H}\alpha)/I(\mathrm{H}\beta)$ ratios were adjusted to the theoretical one by applying a gray shift correction to the red part of the spectrum; the average gray shift was of 0.05 dex and it is due to small displacements of the entrance slits. The accuracy of the line ratios presented in Table 2 is better than 0.04 dex for all the lines with the exception of those lines with a colon, where the accuracy is better than 0.06 dex; the accuracy of $F(\mathrm{H}\beta)$ is better than 0.08 dex and the accuracy of $C(\mathrm{H}\beta)$ is better than 0.1 dex. The H9/Hβ and the H10/Hβ ratios are on the average 0.04 dex and 0.05 dex smaller than predicted which is attributed to the presence of underlying absorption in the continuum due to dust scattered starlight.

Similarly in Table 3 we present the continuum intensities in ergs cm^{-2} s^{-1} A^{-1}, $i(\lambda)$, relative to $I(\mathrm{H}\beta)$ given by

$$\log\,[i(\lambda)/I(\mathrm{H}\beta)] = \log\,[f(\lambda)/F(\mathrm{H}\beta)] + C(\mathrm{H}\beta)g(\lambda) \quad , \qquad (3)$$

where $f(\lambda)$ is the observed continuum flux corrected for atmospheric extinction and where the $C(\mathrm{H}\beta)$ values of Table 2 were used to correct for interstellar extinction. The accuracy of the $i(\lambda)/I(\mathrm{H}\beta)$ ratios is better than 0.06 dex with the exception of the values of M8 HG for which the accuracy is better than 0.04 dex.

The equivalent widths of the emission lines can be obtained from the data presented in Tables 2 and 3. Representative spectra of our data are shown in Figures 2, 3, 4 and 6.

b) *2.1-m at San Pedro Mártir*

The observations were carried out during May 1990 with the spectrograph Boller and Chivens of the University of Milano and a Thompson CS F TH 7883 CDA chip. The CCD has 576 pixels along and 384 pixels perpendicular to the dispersion. A 600 grooves per mm grating blazed at 4550 A was used that covered the 4200 to 5300 A wavelength range. These observations were used to determine the equivalent widths in absorption of the He$^+$ lines in 9 Sgr and H36 and of the λ4430 band in H36 (see Tables 9 and 10).

TABLE 3

CONTINUUM OBSERVATIONS[a]

λ	$g(\lambda)$	$g'(\lambda)$	HG	HGE	HGW	1	1E	1W
3500	+0.375	+0.20	−2.00	−2.08	−1.98	−2.16	−2.10	−2.11
3620	+0.340	+0.19	−2.00	−2.07	−1.99	−2.15	−2.07	−2.09
3930	+0.250	+0.16	−2.44	−2.64	−2.48	−2.71	−2.69	−2.66
4200	+0.175	+0.11	−2.54	−2.77	−2.58	−2.82	−2.79	−2.76
4510	+0.090	+0.06	−2.66	−2.83	−2.68	−2.89	−2.85	−2.83
4800	+0.015	+0.01	−2.73	−2.81	−2.69	−2.87	−2.80	−2.83
6400	−0.305	−0.23	−2.90	−2.68	−2.69	−2.98	−2.91	−2.94

a. log $i(\lambda)/I(\mathrm{H}\beta)$ in A^{-1}.

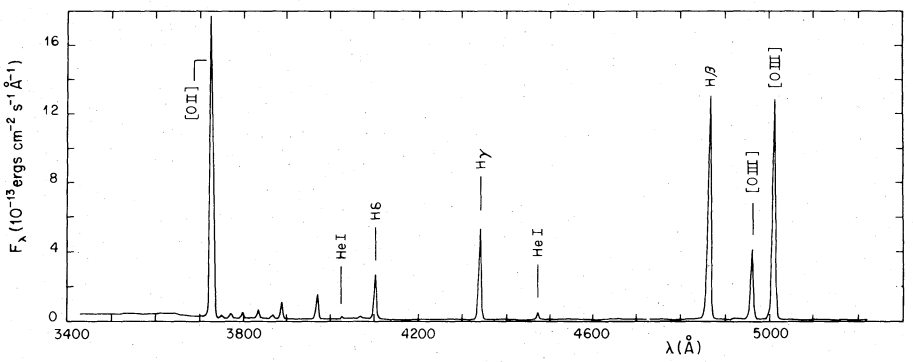

Fig. 2. Blue spectrogram of M8 HG showing the strongest lines measured.

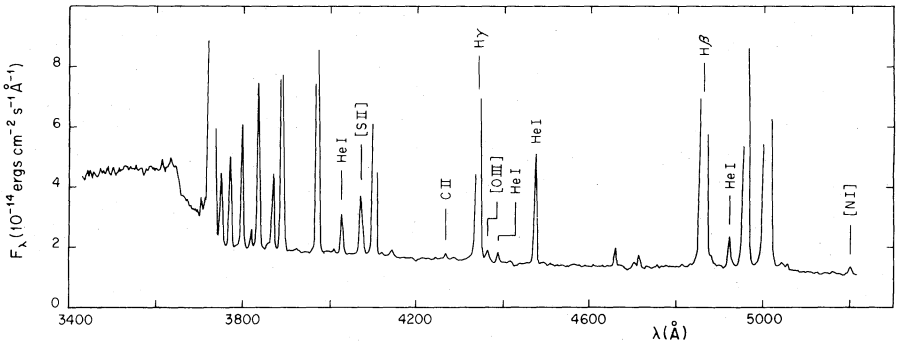

Fig. 3. Blue spectrogram of M8 HG showing the weakest lines measured.

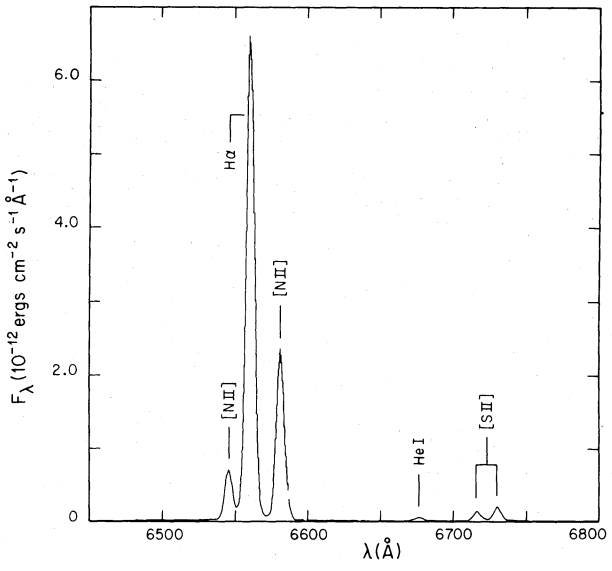

Fig. 4. Red spectrogram of M8 HG, detail in the vicinity of $H\alpha$.

III. PHYSICAL CONDITIONS

a) *Densities and Temperatures*

The atomic parameters needed to derive the electron densities and the electron temperatures were taken from the compilation by Mendoza (1983). The electron densities were derived from the $I(6717)/I(6731)$ line intensity ratios and are presented in Table 4. The density errors in Table 4 correspond to errors in the intensity ratios of 0.02 dex for M8 HG and of 0.04 dex for the other regions.

The T_e(O III) and T_e(N II) values were derived from the $I(4363)/I(5007)$ and the $I(5755)/I(6583)$ ratios respectively and are presented in Table 4. The listed errors in the temperature correspond to errors in the intensity ratios of 0.04 dex for M8 HG and of 0.06 dex for the other regions. Also in Table 4 we present the T_e(O III) and T_e(N II) values for M8 I derived from the observations by Peimbert and Costero (1969) and the newer atomic data available.

The Balmer continuum temperatures, *T(Bac)*,

TABLE 4

DENSITIES AND TEMPERATURES

Region	log N_e(S II)	T_e(Bac)	T_e(O III)	T_e(N II)
HG	$3.35^{+0.15}_{-0.05}$	6600^{+1100}_{-900}	8600±200	8450±300
HGE	< 2.20	6600^{+1800}_{-1300}	8600±300	...
HGW	$2.75^{+0.10}_{-0.25}$	5800^{+1700}_{-1100}	...	...
1	$2.65^{+0.05}_{-0.35}$	7800^{+2100}_{-1500}	8000±300	...
1E	< 2.50	5700^{+1600}_{-1100}	8200±300	...
1W	$3.00^{+0.05}_{-0.20}$	6900^{+1900}_{-1400}	8400±300	...
I	...	...	7850±200	7950±300

were obtained from the ratio of the Balmer continuum, $i(3646, Bac)$, to $I(\mathrm{H})\beta$. To estimate $i(3646,Bac)$ it is necessary to determine the contribution of the other continua to the observed fluxes. For a pure nebular continuum this is done by subtracting the flux of the red side of the discontinuity, $i(3646^+)$, from that of the violet side, $i(3646^-)$, since the intensity variation of the non-Balmer continua should be nil from $\lambda 3646^+$ to 3646^-. Nevertheless in the presence of a contribution to $i(\lambda)$ due to starlight scattered light a small Balmer discontinuity in absorption is expected; Peimbert (1971) has suggested for the Orion nebula that

$$i(3646, Bac) = i(3646^-) - 0.88 i(3646^+), \qquad (4)$$

a similar relation in expected for M8 based on the spectral type of the O stars and on the similar underlying absorption for H9 and H10 in M8 and the Orion nebula (§II and Peimbert 1967). The $i(3646, Bac)$ values were derived by extrapolating the data in Table 3 and from equation (4). To derive the $T_e(Bac)$ values we made use of following equation (Peimbert 1971 and references therein).

$$T_e(Bac) = 2.65 \left[\frac{i(Bac, 3646)}{I(\mathrm{H}\beta)}\right]^{-1.52} ; \qquad (5)$$

in Table 4 we present the $T_e(Bac)$ values where we adopted errors in the $i(Bac, 3646)/I(\mathrm{H}\beta)$ ratios of 0.04 dex for M8 HG and of 0.06 dex for the other regions.

From radio observations Rodríguez and Lichten (1979) obtained $T_e(radio) = 7\,100 \pm 400$ K for M8. We consider that M8 I is representative of M8 due to its location relative to 9 Sgr, that is the main source of ionization, and that T_e(O III) and T_e(N II) of M8 I could be compared with the radio value. For the same reason we also consider representative of M8 the T_e(O III) values derived from M8 HGE and M8 1E.

b) *Average Temperatures and Mean Temperature Variations*

$T_e(Bac)$ and $T_e(radio)$ are smaller than T_e(O III) and T_e(N II) for M8 HG, M8 I, M8 HGE and M8 1E; the differences could be due to the presence of spatial temperature variations along the line of sight. In the presence of spatial temperature variations over the observed volume the methods based on collisionally excited lines yield higher temperatures than those based on recombination lines, free-bound or free-free continua (Peimbert 1967).

We define an average electron temperature, T_0, by

$$T_0(N_i, N_e) = \frac{\int T_e N_i N_e d\Omega dl}{\int N_i N_e d\Omega dl} , \qquad (6)$$

where Ω is the observed solid angle and l is the distance along the line of sight; the root mean square temperature variation, t, is given by

$$t^2 = \frac{\int T_e^2 N_i N_e d\Omega dl - T_0^2 \int N_i N_e d\Omega dl}{T_0^2 \int N_i N_e d\Omega dl} . \qquad (7)$$

It can be shown that (Peimbert 1967)

$$T(Bac) = T_0(1 - 1.70t^2) , \qquad (8)$$

and

$$T(radio) = T_0(1 - 1.42t^2) ; \qquad (9)$$

under the assumption that in the regions where the [O III] and [N II] lines originate T_0 and t^2 are the same it can be shown that

$$T_e(\mathrm{OIII}) = T_0 \left[1 + \frac{1}{2}\left(\frac{90800}{T_0} - 3\right) t^2\right], \qquad (10)$$

and

$$T_e(\mathrm{NII}) = T_0 \left[1 + \frac{1}{2}\left(\frac{69000}{T_0} - 3\right) t^2\right]. \qquad (11)$$

From equations (8) to (11), the T_e values in Table 4 and the $T_e(radio)$ value by Rodríguez and Lichten (1979) the T_0 and t^2 values presented in Table 5 were derived. For M8 HG we used T_e(O III), T_e(N II) and $T_e(Bac)$; for M8 I we used T_e(O III), T_e(N II) and $T_e(radio)$; while for ⟨M8 HGE + M8 1E⟩ we used T_e(O III) and $T_e(radio)$.

We will compare the t^2 values with those predicted by the H II region models of Gruenwald and Viegas (1991), their models compute physical parameters as a function of ξ, the projected distance from the central star in units of the Strömgren radius. M8 HG is mainly ionized by H36 of spectral type O7 (Woolf 1961) or O7.5V(n) (Clayton and Cardelli 1988), while M8 I, M8 HGE and M8 1E are mainly ionized by 9 Sgr of spectral type O5V((f)) (Auer and Mihalas 1972).

We will adopt an O7 spectral type for H36. It is possible to obtain T_0(N II) and T_0(O III) by a linear interpolation of the A3O6 and A3O8 as well as the B3O6 and B3O8 models by Gruenwald and Viegas (1991). The code for the models is such that 3 stands for $N_e = 10^3$ cm^{-3}, A for solar abundances and B for $Z_\odot/3$. From the A models we obtain T_0(N II) = 6375 K and T_0(O III) = 6100 K while from B models we obtain T_0(N II) = 8925 K and T_0(O III) = 8840 K. By looking at Table 5 we find that the T_0 values are in the range defined by A3 and B3 models and again from a linear interpolation to obtain agreement between models and observations we find that T_0(N II) implies Z = 0.67 $Z_\odot$ and T_0(O III) implies Z = 0.76 $Z_\odot$.

The t^2 values in Table 5 can only be compared with the model predictions by Gruenwald and Viegas (1991) for the A2 series ($N_e = 10^2$ cm^{-3}) because they did not publish their t^2 values for the A3 and B3 series. For A2O8 t^2(OIII) can reach values as high as 0.040, but for ξ values higher than 0.2, that apply to M8 HG, t^2(O III) < 0.02. For A2O6 t^2(O III) is smaller than 0.015 for all ξ values. For models A2O6 and A2O8 t^2(N II) is smaller than 0.012 for all ξ values. The predicted t^2 values for models with lower heavy element abundances and higher electron densities, that apply to M8 HG, should be slightly smaller according to the trends present in the models by Gruenwald and Viegas.

The most appropriate models to compare M8 I, M8 HGE and M8 1E are A2O4 and A2O6; these models predict t^2(O III) and t^2(N II) values smaller than 0.015 for all ξ values.

Consequently the t^2 values in Table 5 are higher than those predicted by Gruenwald and Viegas (1991). Peimbert, Sarmiento and Fierro (1991) have obtained a similar result for the Orion nebula and have suggested that the difference could be due to the presence of shock waves inside the H II region. Nevertheless electron temperature determinations of higher accuracy for M8 are needed to corroborate this result.

c) $N(\mathrm{He})^+/N(\mathrm{H})^+$

We derived $N(\mathrm{He})^+/N(\mathrm{H})^+$ values based on the computations by Brocklehurst (1972) and Hummer and Storey (1987). Due to the relatively low N_e and T_e values the collisional contribution from the 2^3S level of He^0 to the λ4472 line is negligible and was not considered (Berrington and Kingston 1987; Clegg 1987; Peimbert and Torres-Peimbert 1987). The results are presented in Table 6, the accuracy in the determinations is of 0.04 dex.

The $N(\mathrm{He})^+/(N(\mathrm{H})^+$ value for M8 HG is smaller than from M8 HGE and M8 1E, the difference is larger than the observational errors and implies that the fraction of helium in the neutral stage is larger

TABLE 5

AVERAGE TEMPERATURES AND MEAN TEMPERATURE VARIATIONS

Region	T_0(O III)	T_0(N II)	t^2(O III)	t^2(N II)
HG	7100±750	7200±750	0.044±0.022	0.051±0.028
I	7300±300	7400±250	0.017±0.009	0.025±0.012
⟨ 1E + HGE ⟩	7400±250	...	0.029±0.016	...

TABLE 6

HELIUM ABUNDANCES

Region	$N(He^+)/N(H^+)$
HG	0.068
HGE	0.099
HGW	0.067
1	0.094
1E	0.088
1W	0.092

or M8 HG than for the other two regions. This esult supports the idea that most of the ionization of M8 HG is due to H36 and the most of the onization of M8 HGE and M8 1E is due to 9 Sgr.

IV. CONTINUUM EMISSION

There are at least five components to the observed continuum emission from a gaseous nebula: 1) contamination due to the night sky, 2) contamination by stars included in the observing slit, 3) electron scattering of starlight, 4) atomic continua and 5) dust scattered starlight.

The night sky contribution was subtracted from the data in Table 3. No star brighter than m_v = +18.5 mag was included in the observed area and we estimate that direct stellar contamination is negligible. The $i(\lambda)/I(H\beta)$ values determined by O'Dell *et al.* (1966) for regions 8 and 9 of M8, that are the regions closest to those observed by us, are −2.79 dex and −2.83 dex respectively, in good agreement with the values presented in Table 3. It can be shown that the electron scattering is negligible for typical H II regions (e.g., Sánchez 1990). We are left with the atomic contribution to the continuum emission, $i(\lambda)_a$, and the dust scattered starlight contribution to the continuum emission, $i(\lambda)_d$. Therefore the continuum emission presented in Table 3 is given by

$$i(\lambda) = i(\lambda)_a + i(\lambda)_d \ . \tag{12}$$

a) *Atomic Continua*

The energy emitted by the atomic continua in the interval $h\nu$ to $h\nu + dh\nu$ may be written as

$$d(energy) = N(H^+)N_e\gamma_{eff}dh\nu dV\,dt \ , \tag{13}$$

where γ_{eff} is expressed in units of a recombination coefficient (cm^3 s^{-1}) and, for a nebula without $N(He^{++})$, is given by

$$\gamma_{eff} = \gamma(H^0) + \gamma(2q) + \\ + \gamma(He^0)N(He^+)/N(H^+) \ , \tag{14}$$

where $\gamma(H^0)$ and $\gamma(He^0)$ include the free-free and free-bound continua of the hydrogen and helium atoms and $\gamma(2q)$ corresponds to the two quantum continuum. The two quantum continuum for T_e = 8000 K is given by (Seaton 1955; Brown and Mathews 1970)

$$\gamma(2q) = \frac{\gamma_0(2q)}{1 + 0.66 \times 10^{-4}N_e} \ . \tag{15}$$

Based on the computations by Seaton (1960) and by Brown and Mathews (1970) we present in Table 7 the atomic continua per unit wavelenght for the low density limit, $N_e \ll 10^4$ cm^{-3}, T_e = 8000 K and

TABLE 7

ATOMIC CONTINUUM[a]

λ	AC_0^b	HG	HGE	HGW	1	1E	1W
3500	−2.25	−2.27	−2.25	−2.26	−2.26	−2.25	−2.26
3620	−2.23	−2.24	−2.23	−2.23	−2.23	−2.23	−2.23
3930	−3.08	−3.12	−3.08	−3.09	−3.09	−3.08	−3.10
4200	−3.13	−3.17	−3.13	−3.14	−3.13	−3.13	−3.14
4510	−3.17	−3.21	−3.17	−3.18	−3.18	−3.17	−3.18
4800	−3.20	−3.23	−3.20	−3.21	−3.20	−3.20	−3.21
6400	−3.25	−3.28	−3.25	−3.27	−3.26	−3.25	−3.26

a. Log $i(\lambda)_a/I(H\beta)$ in A^{-1}. b. For the low density limit and $N(He^+)/N(H^+)$ = 0.10.

$N(He^+)/N(H^+) = 0.10$. The value that we derive for λ4800 A is smaller than that derived by O'Dell *et al.* (1966), probably because they used a higher $N(He^+)/N(H^+)$ ratio. Also in Table 7 we present the atomic continua for the observed regions where the N_e and T_e values in Table 4 and the $N(He^+)/N(H^+)$ values in Table 6 were used.

b) *Dust Scattered Light*

Based on equation (12), Table 3 and Table 7 the dust scattered light to $I(H\beta)$ ratio in presented in Table 8.

TABLE 8

SCATTERED LIGHT[a]

λ	HG	HGE	HGW	1	1E	1W
3500	−2.33	−2.57	−2.30	−2.85	−2.63	−2.64
3620	−2.37	−2.58	−2.36	−2.92	−2.58	−2.65
3930	−2.54	−2.84	−2.60	−2.94	−2.92	−2.86
4200	−2.66	−3.02	−2.72	−3.11	−3.06	−2.99
4510	−2.80	−3.10	−2.85	−3.20	−3.13	−3.09
4800	−2.90	−3.04	−2.85	−3.14	−3.02	−3.06
6400	−3.13	−2.82	−2.82	−3.30	−3.18	−3.22

a. Log $i(\lambda)_d/I(H\beta)$ in A^{-1}.

In Figure 5 we present the dust scattered starlight in M8 HG and compare it with a dereddened O9 star (10 Lac, Code 1960) and with an unreddened black body at 35 000 K. The three spectra are normalized at 4800 A. From Figure 5 it can be seen that M8 HG shows a blue excess and a red excess relative to the other two spectra. The large value of $C(H\beta)$ for H36 (see Table 10) and the larger $C(H\beta)$ value for M8 HG than for the other observed regions (see Table 2) indicate the presence of significant amounts of internal dust. Therefore M8 HG has to be compared with a reddened source; in this case the red excess can disappear but the blue excess becomes larger. This result implies that $A(\lambda)\sigma_d(\lambda)$ the albedo times the average extinction cross section, increases at lower wavelengths.

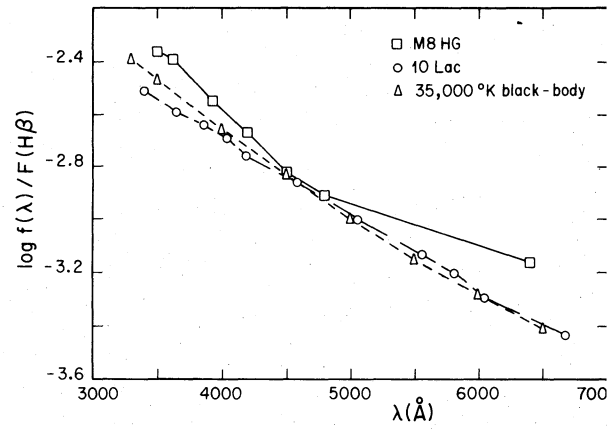

Fig. 5. Comparison of the scattered light in M8 HG with a black body of 35 000 K and 10 Lac. The vertical axis corresponds to M8 HG and the other two curves have been normalized to that of M8 HG at 4800 A.

c) He^+ *Lines in Absorption*

We have detected the $\lambda\lambda$4200 and 4686 He^+ lines in absorption in the direction of M8 HG (see Figure 6). To our knowledge this is the second detection of He^+ absorption lines in the continuum of an H II region, Peimbert and Goldsmith (1972) previously reported the presence of λ4686 in absorption in the direction of the Orion nebula.

In Table 9 we present the observed equivalent widths of $\lambda\lambda$4200, 4542 and 4686 at the M8 HG position. We also present the equivalent widths of

TABLE 9

OBSERVED EQUIVALENT WIDTHS[a]

Object	λ4200	λ4542	λ4686	Sum	Ref.[b]
M8 HG	0.38±0.10	0.13±0.10	0.67±0.10	1.2±0.3	1
9 Sgr	0.66±0.10	0.76±0.10	0.85±0.10	2.3±0.3	1,2
	0.66±0.10	0.85±0.15	0.74±0.15	2.3±0.4	2,3
	0.66±0.10	0.77±0.10	0.82±0.10	2.3±0.3	2,4
H36	0.50±0.10	0.53±0.10	0.75±0.10	1.8±0.3	1,2
15 Mon	0.50±0.10	0.56±0.10	0.71±0.10	1.8±0.3	2,3
	0.50±0.10	0.68±0.10	0.80±0.10	2.0±0.3	2,4

a. Given in A; b. References: 1) this work; 2) Conti 1973; 3) Conti and Alschuler 1971; 4) Auer and Mihalas 1972.

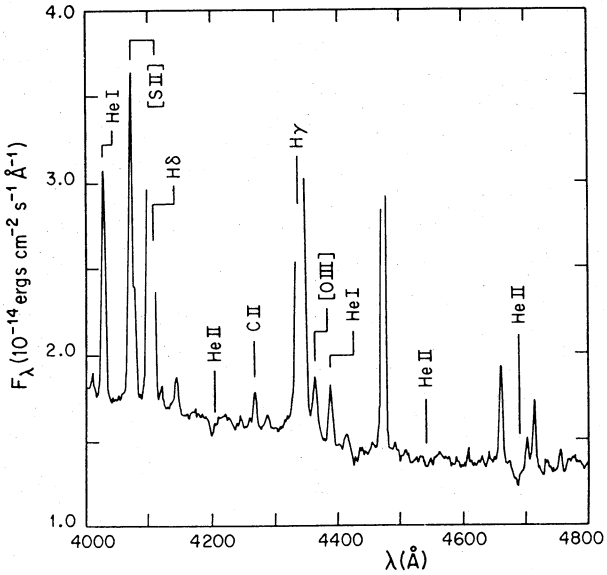

Fig. 6. Blue spectrogram of M8 HG, showing the absorption lines.

H36, 9 Sgr and 15 Mon, an O7V star. Our measurements for H36 and 9 Sgr are in good agreement with those by other observers. The equivalent width of λ4542 is considerably smaller than those of λλ4200 and 4686; probably this is due to the veiling produced by an unidentified emission line in the neighborhood of λ4542.

It is possible to estimate the fraction of dust scattered light by comparing the stellar equivalent widths with those observed in M8 HG. To reduce the errors in this comparison we have used the sum of the three equivalent widths. The ratio of the dust scattered light to the total continuum emission is given by

$$\frac{i_d(\lambda)}{i} = \frac{\sum EW(HG)}{\sum EW(star)} \quad . \qquad (16)$$

For H36 we obtain $i_d/i = 0.67 \pm 0.20$, while for 9 Sgr we obtain $i_d/i = 0.52 \pm 0.15$. The i_d/i ratio derived from the absolute value of the atomic continuum emission in the 4200 to 4800 A range amounts to 0.72 ± 0.06 (see Tables 3 and 8). These results confirm that most of the continuum emission in this part of the spectrum is due to dust scattered starlight, and that H36 is the most probable source of the dust scattered light.

In §V other arguments are given that indicate that H36 is the ionizing source of the Hourglass. There might be a small contribution due to 9 Sgr and Córdoba 12043 to the dust scattered light from M8 HG (Woodward *et al.* 1986). For the other five observed regions it is likely that most of the dust scattered light is due to 9 Sgr.

d) *The Absorption Band at λ4430*

We also marginally detected the absorption band at λ4430 in M8 HG (see Figure 6). In Table 10 we present the equivalent widths and the central absorption depths for the λ4430 band in M8 HG and H36. Our result for H36 is very similar to that derived by Wampler (1966). The central depth of λ4430 might be more representative of the true strength of the band in M8 HG due to the possible presence of faint emission lines close to λ4430.

The strength of λ4430 could be due to the addition of two effects: a) absorption between M8 HG and the observer and b) absorption between H36 and the scattering particles in M8 HG. Without additional observations we can not establish the relative importance of these effects.

TABLE 10

EQUIVALENT WIDTHS, CENTRAL ABSORPTION DEPTH AND LOGARITHMIC REDDENING CORRECTION

Object	λ4430(A)	$P_c(\lambda 4430)(\%)$	$C(H\beta)$	Ref.[a]
M8 HG	0.7±0.2	6.0±1.0	1.00	1
H36	1.2±0.2	6.0±1.0	2.05	1
	...	6.1±0.5	...	2

a. References: 1) This work; 2) Wampler 1966.

V. EFFECTIVE GAS TO DUST RATIO IN THE HOURGLASS

a) *A Simple Model for the Hourglass*

We will consider that the Hourglass is an independent H II region ionized by H36 toward the back of M8 and close to the molecular cloud in the back (e.g., Woodward *et al.* 1986). There are at least four arguments in favor of this proposal: a) H36 is within the boundaries of the Hourglass, while 9 Sgr is at a significantly larger distance; b) the reddening of M8 HG is considerably higher than that of the other observed regions; similarly the reddening of H36 is considerably higher than that of 9 Sgr; c) M8 HG shows a lower degree of ionization than the regions closer to 9 Sgr (see Tables 2 and 6), which is consistent with the later spectral type of H36 relative to that of 9 Sgr; and d) the polarization of the light from the Hourglass is centered on H36 and not on 9 Sgr (Woodward *et al.* 1986).

We will adopt a spherical model for the Hourglass with a radius of 32", which at a distance of 1600 pc (e.g., O'Dell *et al.* 1966; van Altena and Jones 1972; Georgelin and Georgelin 1976) amounts to 0.25 pc, and $N_e(FL) = 2240$ cm^{-3}.

The emission measure of a gaseous nebula is given by

$$EM = \int N_e(\mathrm{rms}) N_p(\mathrm{rms}) dl \ . \qquad (17)$$

From the $I(\mathrm{H}\beta)$ value of M8 HG (see Table 2) and the $\mathrm{H}\beta$ effective recombination coefficient for T_e = 8 000 K, it is obtained that $EM = 1.41 \times 10^6$ cm^{-6} pc, which for l = 0.32 pc and $N(\mathrm{He}^+)/N(\mathrm{H}^+)$ = 0.068 yields an N_e(rms) of 2170 cm^{-3}.

By comparing $N_e(FL)$ and N_e(rms) it is possible to obtain the filling factor from the following equation (e.g., Mallik and Peimbert 1988)

$$\epsilon = N_e^2(\mathrm{rms})/N_e^2(FL) \ , \qquad (18)$$

which for M8 HG is equal to 0.94.

The total number of Lyman continuum photons, $Q(H^0)$, needed to keep ionized a sphere of 0.25 pc, $N_e(FL)$ = 2240 cm^{-3} and ϵ = 0.94 is 1.8×10^{48} s^{-1}. On the other hand, for an O7V star on the zero age main sequence $Q(H^0) = 4.2 \times 10^{48}$ s^{-1}, and for an O8V star on the ZAMS $Q(H^0) = 2.2 \times 10^{48}$ s^{-1} (Panagia 1973); these $Q(H^0)$ values are consistent with the idea that the ionization of the Hourglass is due to H36.

Woodward *et al.* (1986) obtain $Q(H^0) = 1.9 \times 10^{48}$ s^{-1} from a different geometrical model of the Hourglass, and conclude that the ionization is due to H36.

b) *Total Extinction Method*

The total extinction at $\mathrm{H}\beta$ produced inside an H II region is given by

$$C(\mathrm{H}\beta)_{INT} = 0.4343 N_d \sigma_d(\mathrm{H}\beta) \epsilon l \ , \qquad (19)$$

where N_d is the number of dust particles per unit volume in the nebula, $\sigma_d(\mathrm{H}\beta)$ is their average extinction cross section at $\mathrm{H}\beta$ and l is the length of the nebula along the line of sight. Therefore the effective gas to dust ratio is given by

$$\frac{N_p(FL)}{N_d \sigma_d(\mathrm{H}\beta)} = 0.4343 N_p(FL) \epsilon l / C(\mathrm{H}\beta)_{INT} \ . \qquad (20)$$

The observed $C(\mathrm{H}\beta)$ value in the direction of M8 HG is due to a foreground contribution, $C(\mathrm{H}\beta)_{FOR}$, plus the extinction due to the Hourglass, i.e.,

$$C(\mathrm{H}\beta)_{OBS} = C(\mathrm{H}\beta)_{FOR} + C(\mathrm{H}\beta)_H \ . \qquad (21)$$

Based on the $C(\mathrm{H}\beta)_{OBS}$ values for HGE and HGW we will assume for M8 HG that $C(\mathrm{H}\beta)_{FOR}$ = 0.45; consequently based on the $C(\mathrm{H}\beta)$ determined from the Balmer decrement, which is practically the same as the $C(\mathrm{H}\beta)$ determined from the comparison of the free-free radio emission with $F(\mathrm{H}\beta)$, it follows that $C(\mathrm{H}\beta)_H$ = 0.55.

$C(\mathrm{H}\beta)_H$ is equal to $C(\mathrm{H}\beta)_{INT}$ only if all the dust of the Hourglass is in front of it. In this case $C(\mathrm{H}\beta)_H = C(\mathrm{H}\beta)_{INT}$ = 0.55, which from equation (20) yields an effective gas to dust ratio of 1.71×10^{21} cm^{-2}.

For the case where the albedo is zero and the (gas emission)/(dust absorption) is uniform it can be shown that

$$e^{-\tau_H} = \frac{1 - e^{-\tau_{INT}}}{\tau_{INT}} \ , \qquad (22)$$

where τ is the optical depth, and is equivalent to

$$C(\mathrm{H}\beta)_H = -\log_{10}\left[0.4343 \frac{1 - 10^{-C(\mathrm{H}\beta)_{INT}}}{C(\mathrm{H}\beta)_{INT}}\right] , \qquad (23)$$

which for $C(\mathrm{H}\beta)_H \ll 1$ yields

$$C(\mathrm{H}\beta)_H = \frac{1}{2} C(\mathrm{H}\beta)_{INT} \ . \qquad (24)$$

From $C(\mathrm{H}\beta)_H$ = 0.55 and equation (22) it follows that $C(\mathrm{H}\beta)_{INT}$ = 1.49; therefore from equation (20) the effective gas to dust ratio for the Hourglass becomes 6.3×10^{20} cm^{-2}.

Mathis (1970) has also obtained that the observed interstellar extinction is only a fraction of the true internal extinction for models with albedo different from zero.

We will compare the effective gas to dust ratios of the Hourglass with those derived for M8 and the general field based on the total extinction method. For M8 O'Dell *et al.* (1966) obtain 2.12×10^{21} cm^{-2}; this value could increase if part of the extinction is produced in front of M8, alternatively according to equations (20) and (22) this value could decrease if the gas is mixed with the dust. O'Dell *et al.* (1966) obtained 2.0×10^{21} cm^{-2} for the effective gas to dust ratio of the general field, while Bohlin, Savage and Drake (1978) obtained 3.5×10^{21} cm^{-2}, where it has been assumed that their measurement involved scattering with an albedo of 0.5. These two values are considerably higher than the

value derived from equation (22) for the Hourglass probably implying either that there are intrusions of neutral gas and dust mixed with the ionized gas in the Hourglass, or that most of the dust responsible for $C(\mathrm{H}\beta)$ is in the outer regions of the Hourglass in our direction, or that there is a density gradient decreasing towards the observer, but with $N(\mathrm{dust})/N(\mathrm{gas})$ = constant. In this latter case the emission would then be concentrated towards the back of the nebula ($\propto N^2$), with the dust relatively in front ($\propto N$), so there would be more absorption per H atom than "normal".

We note that the spread in the effective gas to dust ratios, of about a factor of three between the general field value and the ρ Oph value, derived from selective extinction measurements (Savage and Mathis 1979) becomes considerably reduced if to estimate the amount of dust the total extinction is used instead of the selective extinction.

c) *Scattering Method*

The effective gas to dust ratio of an optically thin spherical H II region illuminated by a central source is given by (O'Dell *et al.* 1966; Osterbrock 1989)

$$\frac{N_p(FL)}{A(\lambda)N_d\sigma_d(\lambda)} = \frac{I(\mathrm{H}\beta)}{i_d(\lambda)} \frac{1}{N_e(FL)\alpha(\mathrm{H}\beta)h\nu(\mathrm{H}\beta)} \frac{L^*(\lambda)}{4\pi D^2} \times \times \frac{D^2 \cos^{-1}(b/r_0)}{r_0 r_1 (b/r_0)\,[1-(b/r_1)^2]^{1/2}}, \quad (25)$$

where A is the albedo, $\alpha(\mathrm{H}\beta)$ the effective recombination coefficient, r_0 the radius of the dust cloud, r_1 the radius of the ionized gas, b the minimum projected distance from the observing point to the central star ($b/r_1 = \xi$), and L^* the luminosity of the central star.

For the Hourglass: D = 1600 pc, b = 0.19 pc and $r_0 = r_1$ = 0.25 pc. For an unreddened O7V star $L^*(4800)$ is equal to 2.00×10^{-11} erg cm^{-2} s^{-1} A^{-1} (Code 1960; Panagia 1973). From equation (25) evaluated at λ = 4800 we obtain an effective gas to dust ratio equal to 2.78×10^{21} cm^{-2}.

Mathis (1971) has obtained an expression equivalent to equation (25) where the assumption of an optically thin nebula has been dropped. For reasonable values of $A(\mathrm{H}\beta)$ and $\tau(\mathrm{H}\beta)_{INT}$ he obtains results that differ by less than a factor of two from those of the optically thin case.

Mathis (1971) has noted that in the presence of spatial density fluctuations if N_e(rms) is used in equation (25) the effective gas to dust ratio is overestimated by $\epsilon^{-1/2}$, see equation (18).

We also present in Table 11 the effective gas to dust ratios derived by O'Dell *et al.* (1966) for M8 assuming that it is optically thin, and those derived by Mathis (1971) considering the radiative transfer problems due to reasonable values of A and $\tau(\mathrm{H}\beta)_{INT}$. These values are similar to the result obtained for the Hourglass from equation (25).

TABLE 11

EFFECTIVE GAS-TO-DUST RATIO

Object	$N_H/N_d\sigma_d$ (10^{21} cm^{-2})	Method	Ref.[a]
Hourglass	1.71	Total Extinction[b]	1
	0.63	Total Extinction[c]	1
	2.78	Scattering	1
M8	2.12	Total Extinction	2
	2.30	Scattering	2
	1.9	Scattering (ϕ_d = 30')	3
	4.0	Scattering (ϕ_d = 40')	3
General Field	2.0	Total Extinction	2
	3.5	Selective Extinction	4

a. References: 1) this work; 2) O'Dell *et al.* 1966; 3) Mathis 1971; 4) Bohlin *et al.* 1978. b. Dust in front. c. Dust mixed with gas.

VI. CONCLUSIONS

The t^2 values derived for M8 are larger than predicted by photoionization models. This result probably implies that there are additional energy sources present in M8, like stellar winds.

The geometry, the degree of ionization of M8 HG and the value of reddening in the direction of M8 HG, higher than in the direction of the other observed regions, support the idea that the Hourglass is mainly ionized by H36.

The nebular atomic continua were computed for the six observed regions and are considerably smaller than the observed nebular continua; the difference was attributed to dust scattered starlight.

The He^+ lines $\lambda\lambda$4200 and 4686 are seen in absorption in the direction of M8 HG indicating that most of the light in the blue region is due to dust scattered light, in agreement with the result derived from the contribution of the atomic continua to the observed nebular continuum.

The albedo times the average extinction cross section, $A(\lambda)\sigma_d(\lambda)$, increases at lower wavelengths for all the observed regions.

The effective gas to dust ratio for the Hourglass, determined from the total extinction method is equal to 6.3×10^{20} cm^{-2}. This result is based on the assumptions that the gas and the dust are well mixed and that there are no regions of neutral hydrogen in the Hourglass. This value is considerably smaller than that of the general field,

and probably implies that some of the assumptions made in its determination are poor.

We obtained an effective gas to dust ratio of 2.78 $\times 10^{21}$ cm^{-2} for the Hourglass based on a simple model and on the observed scattered light. This result is similar to that derived for M8 by other authors based on the same method; it also supports the idea that most of the ionization of the Hourglass is due to H36.

It is a pleasure to acknowledge S. Torres-Peimbert for helping us to gather the observations presented in this paper. We are grateful to the referee for several excellent suggestions. L.J.S. received economic support from Sistema Nacional de Investigadores SEP during the preparation of this article.

REFERENCES

Auer, L.H., & Mihalas, D. 1972, ApJS, 24, 193
Berrington, K.A., & Kingston, A.E. 1987, J.Phys.B., 20, 6631
Bohlin, R.C., Savage, B.D., & Drake, J.F. 1978, ApJ, 224, 132
Brocklehurst, M. 1971, MNRAS, 153, 471
____. 1972, MNRAS, 157, 211
Brown, R.L., & Mathews, W.G. 1970, ApJ, 160, 939
Clayton, G.C., & Cardelli, J.A. 1988, AJ, 96, 695
Clegg, R.E.S. 1987, MNRAS, 229, 31p
Code, A.D. 1960, in Stellar Atmospheres, Vol. VI of Stars and Stellar Systems, ed. J.L. Greenstein (Chicago: University of Chicago Press), p.50
Conti, P.S. 1973, ApJ, 179, 161
Conti, P.S., & Alschuler, W. 1971, ApJ, 170, 325
Georgelin, Y.M., & Georgelin, Y.P. 1976, A&A, 49, 57
Gruenwald, R.B., & Viegas, S.M. 1991, ApJS, in press
Hecht, J., Helfer, H.L., Wolf, J., Donn, B., & Pipher, J.L. 1982, ApJ, 263, L39
Hummer, D.G., & Storey, P.J. 1987, MNRAS, 224, 801
Lada, C.J., Gull, T.R., Gottlieb, C.A., & Gottlieb, E.W. 1976, ApJ, 203, 159
Mallik, D.C.V., & Peimbert, M. 1988, RevMexAA, 16, 111
Mathis, J.S. 1970, ApJ, 159, 263
____. 1971, ApJ, 167, 261
____. 1990, ARA&A, 28, 37
Mendoza, C. 1983, in Planetary Nebulae, IAU Symposium No. 103, ed. D.R. Flower (Dordrecht: D. Reidel), p. 143
O'Dell, C.R., & Hubbard, W.B. 1965, ApJ, 142, 591
O'Dell, C.R., Hubbard, W.B., & Peimbert, M. 1966, ApJ, 143, 743
Oke, J.B. 1974, ApJS, 27, 21
Osterbrock, D.E. 1989, Astrophysics of Gaseous Nebulae and Active Galactic Nuclei (California: University Science Books)
Panagia, N. 1973, AJ, 78, 929
Peimbert, M. 1967, ApJ, 150, 825
____. 1971, Bol. Obs. Tonantzintla Tacubaya, 6, 29
Peimbert, M., & Costero, R. 1969, Bol. Obs. Tonantzintla Tacubaya 5, 3
Peimbert, M., & Goldsmith, D.W. 1972, A&A, 19, 398
Peimbert, M., & Torres-Peimbert, S. 1987, RevMexAA, 14, 540
Peimbert, M., Sarmiento, A., & Fierro, J. 1991, PASP, 103, 815
Rodríguez, L.F., & Lichten, S.M. 1979, Ap. Lett., 20, 37
Sánchez, L.J. 1990, B. Sc. Thesis, Universidad Nacional Autónoma de México
Savage, B.D., & Mathis, J.S. 1979, ARA&A, 17, 73
Seaton, M.J. 1955, Proc. Roy. Soc. London, A, 68, 457
____. 1960, Rept. Progr. Phys., 23, 313
Stone, R.P.S. 1977, ApJ, 218, 767
van Altena, W.F., & Jones, B.F. 1972, A&A, 20, 425
Wampler, E.J. 1966, ApJ, 144, 921
Whitford, A.E. 1958, AJ, 63, 201
Woodward, C.E., Pipher, J.L., Helfer, H.L., Sharpless, S., Moneti, A., Kozikowski, D., Oliveri, M., Willner, S.P., Lacasse, M.G., & Herter, T. 1986, AJ, 91, 870
Woolf, N.J. 1961, PASP, 73, 206

Leonardo J. Sánchez and Manuel Peimbert: Instituto de Astronomía, UNAM, Apartado Postal 70-264, 04510 México, D.F., México.

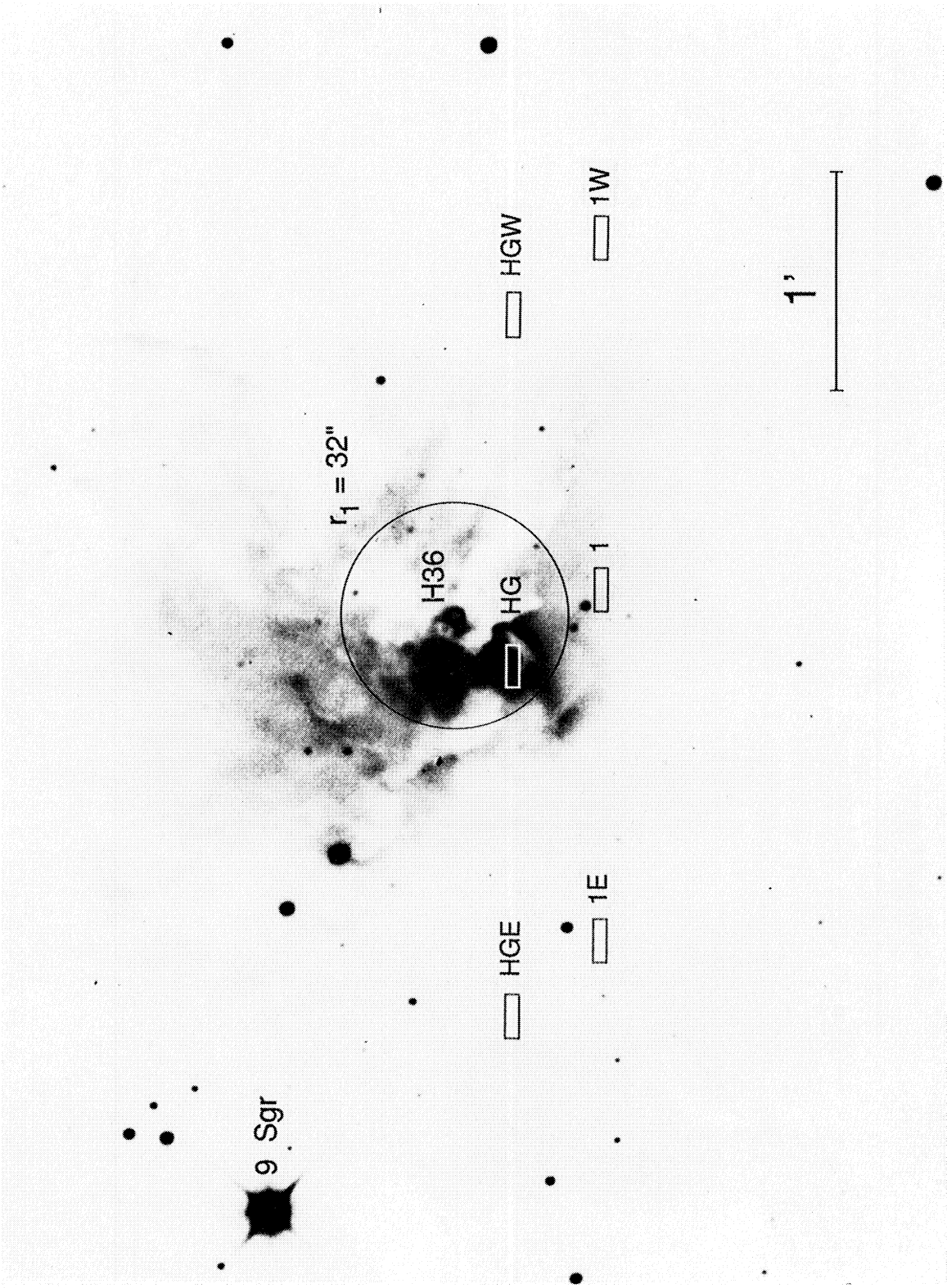

Fig. 1. Observed Regions and a circle of 32" centered on H36 are superposed on a photograph obtained with the 3-m Shane telescope (Lick Observatory photograph).